

Investigations into *SCAMP5*, a candidate lupus risk gene expressed in plasmacytoid dendritic cells

Mustafa H Ghanem ^{1,2}, Andrew J Shih ¹, Himanshu Vashistha ¹,
Latanya N Coke ¹, Wentian Li ¹, Sun Jung Kim ^{1,2},
Kim R Simpfendorfer ^{1,2}, Peter K Gregersen ^{1,2}

To cite: Ghanem MH, Shih AJ, Vashistha H, *et al.* Investigations into *SCAMP5*, a candidate lupus risk gene expressed in plasmacytoid dendritic cells. *Lupus Science & Medicine* 2021;**8**:e000567. doi:10.1136/lupus-2021-000567

► Additional supplemental material is published online only. To view, please visit the journal online (<http://dx.doi.org/10.1136/lupus-2021-000567>).

KRS and PKG are joint senior authors.

Received 25 August 2021
Accepted 1 October 2021



© Author(s) (or their employer(s)) 2022. Re-use permitted under CC BY-NC. No commercial re-use. See rights and permissions. Published by BMJ.

¹The Institute of Molecular Medicine, Northwell Health Feinstein Institutes for Medical Research, Manhasset, New York, USA

²Donald and Barbara Zucker School of Medicine at Hofstra/Northwell, Hempstead, New York, USA

Correspondence to

Dr Peter K Gregersen;
pgregers@northwell.edu
and Dr Kim R Simpfendorfer;
ksimpfendo@northwell.edu

ABSTRACT

Objective We have investigated the molecular function of *SCAMP5*, a candidate risk gene for SLE exclusively expressed in plasmacytoid dendritic cells (pDCs) among peripheral leucocytes.

Methods We tested the independence of the association in *SCAMP5* with SLE by performing conditional analyses. We profiled the expression pattern of *SCAMP5* among circulating leucocytes at the transcript and protein levels. Using lentiviral vectors, we localised the subcellular distribution of *SCAMP5* alongside the interferon secretory pathway. We analysed pDCs for the expression of *SCAMP5* and interferon production capacity by *SCAMP5* genotype. Finally, we examined pDC-specific *SCAMP5* isoforms by total RNAseq analysis and examined for genotype-associated quantitative differences therein.

Results A conditional analysis revealed evidence of an independent genetic association of *SCAMP5* with SLE. Among circulating leucocytes, *SCAMP5* is uniquely expressed in pDCs at the transcript and protein levels, with main presence in the Golgi apparatus and minor presence at the cell periphery. In live cells, *SCAMP5* displayed dynamic Golgi-cell surface trafficking and localised with the interferon secretory pathway. *SCAMP5* did not differ in expression levels in pDCs between genotyped donors; however, a transient interferon secretory defect was noted in pDCs from donors carrying the risk genotype.

Conclusions *SCAMP5* constitutes a novel SLE risk gene on the basis of genomic data and expression in a cell type widely implicated in SLE pathogenesis. While we could not find evidence of quantitative expression differences in *SCAMP5* between genotyped donors, *SCAMP5* remains an attractive gene to explore given its highly restricted expression pattern and colocalisation with interferon secretion.

INTRODUCTION

Plasmacytoid dendritic cells (pDCs) are rare innate immune cells which express the pattern recognition receptors toll-like receptors 7 and 9 (TLR7 and TLR9), which together with their constitutive expression of the type I interferon (IFN-I) inducer interferon regulatory factor 7 (IRF7) are poised to rapidly respond to viral infection.¹ Secretion

KEY MESSAGES

WHAT IS ALREADY KNOWN ABOUT THIS SUBJECT?

⇒ SLE is associated with overactivity of the type I interferon pathway, and plasmacytoid dendritic cells (pDCs) are major producers of type I interferon in this disease.

WHAT DOES THIS STUDY ADD?

- ⇒ A polymorphism on chromosome 15q24 associates with SLE by virtue of a novel candidate SLE risk gene, *SCAMP5*.
- ⇒ We confirmed that among circulating leucocytes, *SCAMP5* is uniquely expressed in pDCs at the transcript and protein levels, with main presence in the Golgi apparatus and minor presence at the cell periphery.
- ⇒ We detected a transient interferon secretory defect in pDCs from donors homozygous for the SLE risk genotype, providing a potential link between a functional consequence of the genetic risk variant and the SLE risk association.

HOW MIGHT THIS IMPACT ON CLINICAL PRACTICE OR FUTURE DEVELOPMENTS?

⇒ Molecular dissection of heritable traits in type I interferon secretion may unveil novel opportunities for drug development.

of massive amounts of IFN-I, particularly IFN- α , is characteristic of pDCs, and downstream signalling in response to IFN drives induction of an antiviral programme in host cells, an 'IFN signature' that is constitutively activated in the blood of many patients with SLE.²

A role of pDCs in the pathogenesis of SLE has also been suggested by their presence in cutaneous lupus lesions and in lupus nephritis.^{3,4} Furthermore, antibody-mediated depletion of pDCs has demonstrated therapeutic efficacy in human trials.⁵ From the genomic standpoint, several SLE risk genes are enriched for expression in pDCs, including *TLR7*, *IRF7*, *IRF8* and *DNASE1L3*.^{6,7}

pDC production of IFN-I is potentially a major driver of the IFN signature. IFN-I signalling has been shown to enhance antigen presentation, promote B cell differentiation and suppress regulatory T cells—processes central to the development of SLE.^{8–10}

In their recent meta-analysis of genomewide association studies (GWAS) of SLE, Bentham *et al*¹¹ reported an association at single-nucleotide polymorphism (SNP) rs2289583, with an OR of 1.19 and a *p* value of 6×10^{-15} . rs2289583 occurs in intron 6 of *SCAMP5*, a member of the secretory carrier membrane protein (SCAMP) family. The SCAMPs are tetraspan membrane proteins with cytoplasmic N-termini and C-termini and both luminal and extraluminal peptide loops connecting the transmembrane domains along the surface of intracellular trafficking vesicles (online supplemental figure S1).¹² SCAMPs 1–3 are ubiquitously expressed, whereas SCAMPs 4–5, lacking the characteristic N-terminal NPF repeats of the other SCAMPs, display a more limited expression pattern, largely restricted to the brain.¹³ This expression profile of *SCAMP5* in the central nervous system appears to be conserved among mammalian species.

Outside of the brain, we noted a strong signal for *SCAMP5* expression in pDCs.¹⁴ Given the multiplicity of evidence for the role played by pDCs in SLE, and the association of this risk locus with the disease, we sought to determine whether *SCAMP5* contributed to SLE by modulating a key function of pDC biology: IFN-I secretion.

METHODS

See online supplemental material.

RESULTS

SCAMP5 associates independently with SLE on chr15q24

A recent SLE GWAS meta-analysis reported on susceptibility loci concentrated in genes involved in innate and adaptive immune function.¹¹ This study coupled analyses of their respective discovery and replication cohorts with a previous SLE GWAS from our group.¹⁵ Among the associations was the polymorphism rs2289583. *CSK* was annotated as the likely gene explaining the association signal, citing prior work from our group establishing a link between *CSK* and SLE in this genomic region.¹⁶

However, inspection of SNP associations across this region reveals that the lead SNP from this analysis lies within the *SCAMP5* gene, ~155 kb telomeric to *CSK*. This raised the question as to whether *CSK* drives the association signal at rs2289583. We examined the primary data in this region, with individual-level data on 4036 SLE cases and 6959 controls from the main GWAS of the aforementioned study.¹¹ As shown in figure 1A (left panel), two SNPs associated with SLE risk achieve genome-wide significance in the region: rs2289583 in the last intron of *SCAMP5* (OR=1.2, $p=3.4 \times 10^{-9}$) and rs1378940 in the first intron of *CSK* (OR=1.17, $p=2.8 \times 10^{-8}$). Our group previously identified B cell phenotypes associated with a lupus risk variant in the *CSK* gene (rs34933034).¹⁶ The rs34933034 SNP was not

genotyped in the Bentham *et al* data set. In fact, this variant in *CSK* is poorly imputed by other variants in the region—the lead SNP in *CSK* in this analysis (rs1378940) exhibits an $r^2=0.34$ with rs34933034. Moreover, the signal at rs2289583 is unlikely to reflect the effects of our previously identified association at *CSK*, as the linkage disequilibrium (LD) between these two SNPs is also quite modest ($r^2=0.2$ between rs34933034 and rs2289583).

Therefore, we carried out formal conditional analysis to seek evidence for *SCAMP5* as a secondary or alternative driver of the SLE risk association in the *CSK/SCAMP5* region. On conditioning on the associated SNP within *SCAMP5*, the signal at rs1378940 within *CSK* is substantially reduced (figure 1A, middle panel). In contrast, the association signal in *SCAMP5* (rs2289583 OR=1.2, $p=3.4 \times 10^{-9}$) was only partially reduced following conditioning on the lead risk-association SNP in *CSK* ($p_{\text{cond}}=1.66 \times 10^{-4}$) (figure 1A, right panel), indicating that the signal at *SCAMP5* is independent of the association signals observed within *CSK* itself.

SCAMP5 is uniquely expressed in pDCs among peripheral blood leucocytes

Having established that *SCAMP5* may represent a novel SLE risk gene, we sought to probe the functional biology underlying this association. *SCAMP5* is reported to be expressed uniquely by pDCs among peripheral blood leucocytes in humans (BioGPS¹⁷ and Human Protein Atlas¹⁴; online supplemental figure S2). To confirm this, we sorted leucocyte subsets from four healthy donors and examined *SCAMP5* expression by reverse transcription (RT)-PCR. *SCAMP5* transcript was detected in pDCs from all donors and was absent in their B, T and NK cells, as well as monocytes and conventional dendritic cells (cDCs) (figure 1B, left panel). To determine whether *SCAMP5* is expressed at the protein level in pDCs, we resolved lysates from several leucocyte subsets and detected *SCAMP5* protein using the polyclonal antibody (pAb) against *SCAMP5* employed by the Human Protein Atlas. We found that *SCAMP5* is indeed expressed at the protein level only in pDCs (figure 1B, middle panel). To agnostically determine whether any other (unsorted) peripheral blood leucocyte subset expressed *SCAMP5*, RBC-depleted whole blood was stained intracellularly for *SCAMP5* using the same pAb. Only pDCs stained for *SCAMP5*, confirming the unique expression of this protein in the circulation (figure 1B, right panel).

To localise expression of *SCAMP5* within pDCs, fixed and permeabilised pDCs were stained for *SCAMP5* and visualised by immunofluorescence. Colocalisation was evident with the Golgi marker golgin-97, with additional evidence of staining for *SCAMP5* at the cell periphery (figure 1C).

The novelty of *SCAMP5* as an SLE risk gene, coupled with the striking expression pattern restricted to pDCs, a cell type highly invoked in SLE pathogenesis, prompted us to further explore a role of *SCAMP5* in modulating pDC function.

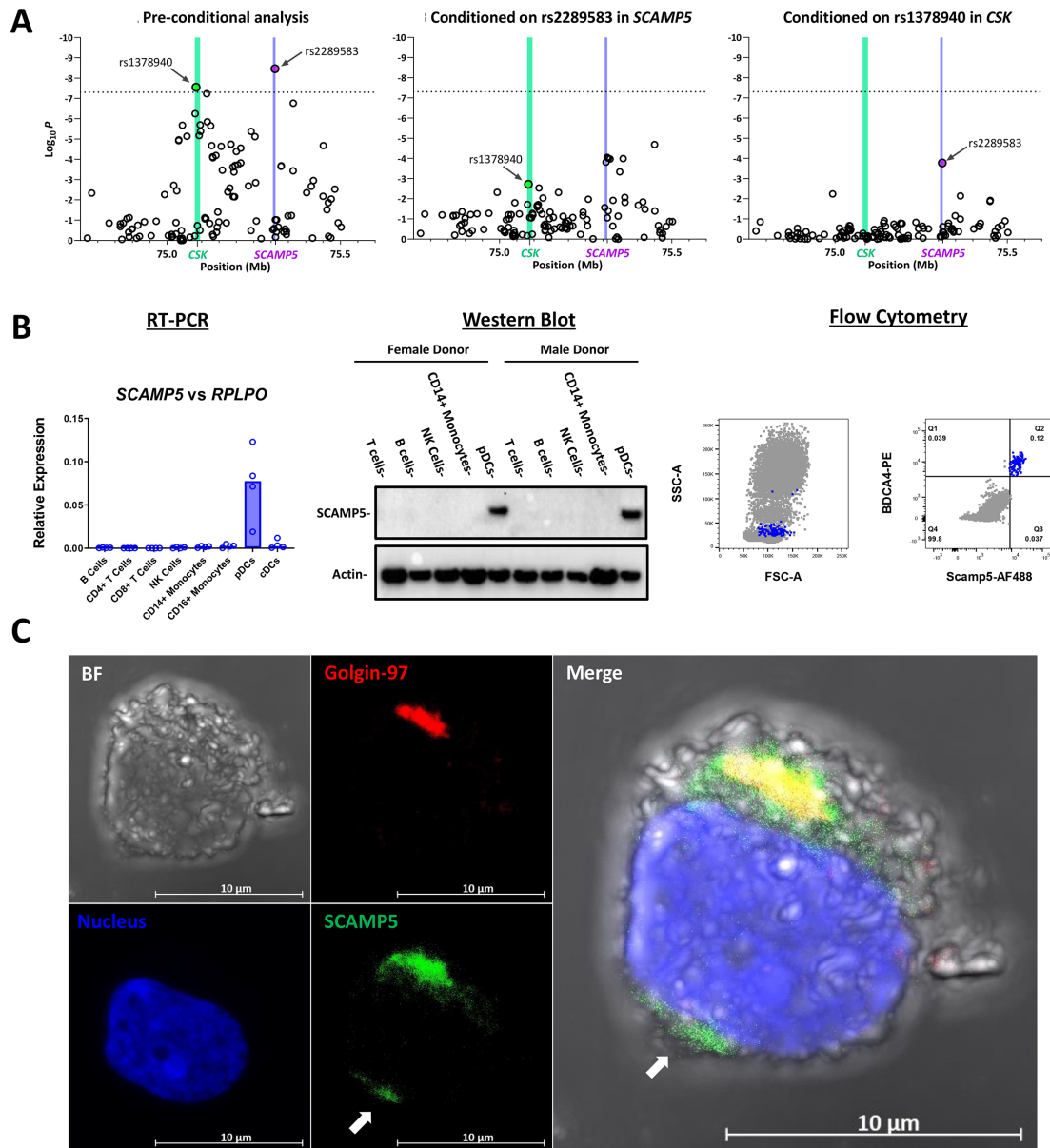


Figure 1 SCAMP5 associates independently with SLE and is expressed in the Golgi apparatus and cell periphery of pDCs. (A) Genomic coordinates and conditional analyses on lead SLE association SNPs in SCAMP5 and CSK. (Left) Summary of SNP associations in the CSK-SCAMP5 region on chromosome 15 from Bentham *et al*¹¹ for 4036 SLE cases and 6959 controls. The association values following conditioning on the lead risk-association SNP in SCAMP5 (rs2289583 in purple) (middle) or the lead risk-association SNP in CSK (rs1378940 in green) (right). Genome-wide significance at 5×10^{-8} is indicated by the dotted line. Vertical shading depicts the location of the SCAMP5 gene (purple) and CSK gene (green). Positions are from the 2009 (GRCh37/hg19) assembly. (B) SCAMP5 is expressed exclusively in pDCs among human circulating leucocytes. (Left) Quantitative RT-PCR for SCAMP5 reveals significant expression in pDCs and not in lymphocytes, monocytes or cDCs. Each data point represents one donor's flow sorted cells. (Middle) Likewise, SCAMP5 protein is detected by a specific antibody in pDCs and not in other immune cells in western blot. (Right) Intracellular labelling for SCAMP5 in RBC-depleted human whole blood analysed by flow cytometry indicates that SCAMP5 is present in the small population of BDCA4hi cells (pDCs) and absent in all other cells in the circulation, including the granulocyte population as reflected by light scatter. (C) Subcellular immunolocalisation of SCAMP5 in pDCs. Representative confocal Z-stack maximal projection image of a pDC stained for SCAMP5 and a Golgi-resident membrane protein, golgin-97. SCAMP5 concentrates in the Golgi, with minor presence at the cell periphery (arrow). 63× magnification with oil immersion. Staining with DAPI delineates the nucleus. cDCs, conventional dendritic cells; pDCs, plasmacytoid dendritic cells; RT-PCR, reverse transcription PCR.

SCAMP5 traffics between the Golgi stack and cell surface and colocalises with clathrin and the IFN-I export pathway

The SCAMP protein family remains understudied. To develop tools to enable a more complete understanding

of SCAMP5 in particular, several SCAMP5 constructs were generated and cloned into lentiviral vectors. To localise and track SCAMP5 in live cells, a SCAMP5-mKate2 fusion protein was designed. SCAMP5-mKate2 was transduced

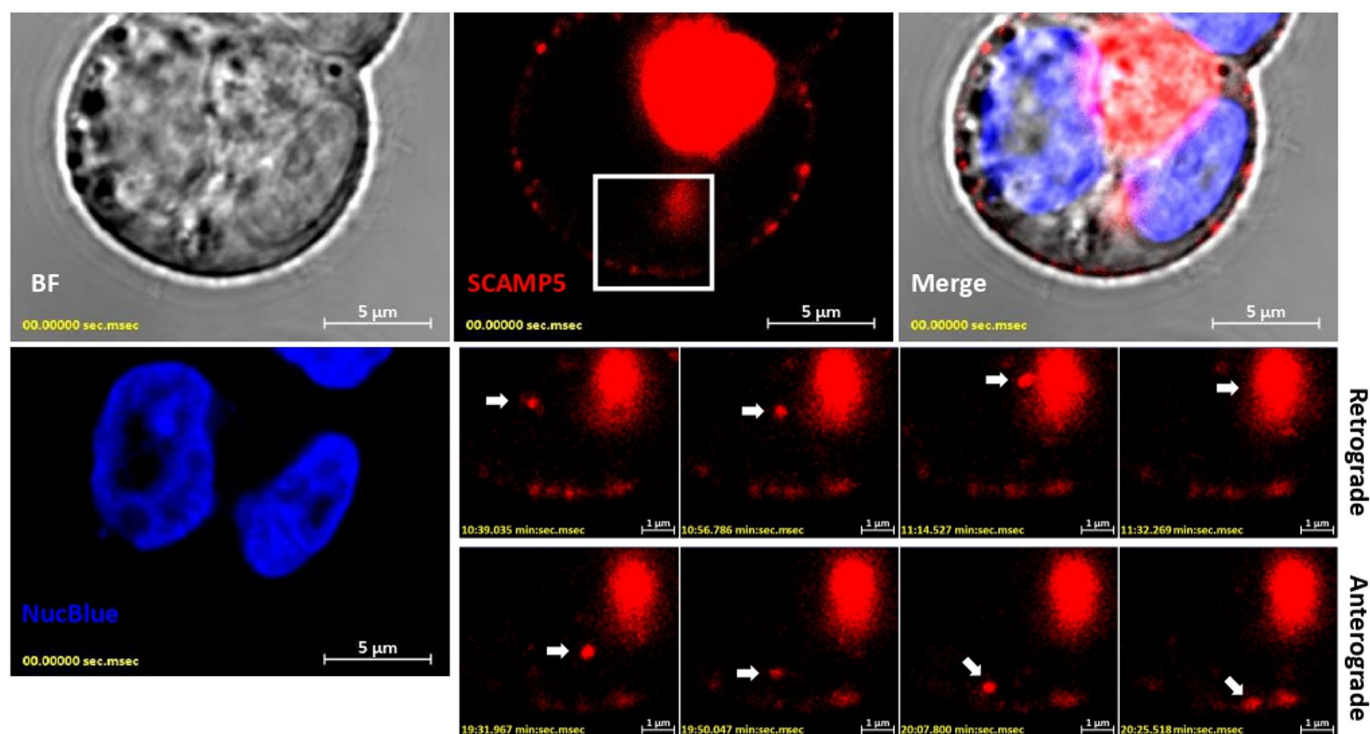


Figure 2 Live cell imaging of SCAMP5 intracellular trafficking. HEK cells transduced with a lentiviral vector to express SCAMP5-mKate2 were imaged by time-lapse confocal microscopy. SCAMP5 was predominantly localised to the Golgi apparatus. Additional SCAMP5 puncta were present at the cell periphery (similar distribution to that observed in figure 1C). Intracellular vesicles bearing SCAMP5 were observed to traffic in both anterograde and retrograde directions between the cell surface and the Golgi (lower right images representing the magnified region indicated by the white box, white arrows trace a unique vesicle across acquisition intervals in the retrograde (upper panels) and anterograde (lower panels) trajectories). See online supplemental materials online supplemental files for SCAMP5-mKate2 construct design. Correlate with online supplemental video 1, online supplemental video 2, online supplemental video 3, online supplemental video 4. 63× magnification with oil immersion. NucBlue delineates the nucleus. BF, bright-field; HEK, human embryonic kidney.

into human embryonic kidney (HEK) cells. SCAMP5-mKate2 localised mainly to the Golgi body, with puncta observed at the cell periphery (figure 2). This distribution matched the SCAMP5 localisation patterns observed by immunofluorescence on endogenously expressed SCAMP5 in primary pDCs (figure 1C). On time-series imaging, SCAMP5 was highly motile in the cell, with both anterograde and retrograde trajectories observed between the Golgi and the plasma membrane (figure 2 and online supplemental video 1, online supplemental video 2, online supplemental video 3, online supplemental video 4).

To probe for a possible interaction between SCAMP5 and the IFN- α trafficking pathway, the fluorescent protein mVenus was generated as a soluble expression construct, designated 'cytosolic/c-mVenus' or with the signal peptide from human IFN- α at the N-terminus (designated 'IFNsp-mVenus'). Both c-mVenus and IFNsp-mVenus were cloned downstream of a doxycycline-inducible promoter. Expression of c-mVenus in HEK cells revealed a fluorescence pattern that was diffusely present in the cytoplasm, as expected, including in lamellipodia. IFNsp-mVenus displayed a more restricted fluorescence pattern, highlighting the endoplasmic reticulum (ER) throughout the cell (figure 3A and online supplemental video 5,

online supplemental video 6). Both c-mVenus and IFNsp-mVenus were induced in a doxycycline dose-responsive manner. IFNsp-mVenus was detected in the culture media and cell lysates, whereas expression of c-mVenus was only detectable in cell lysates (figure 3B), demonstrating that IFNsp-mVenus was actively secreted. Coexpression of IFNsp-mVenus with SCAMP5-mKate2 demonstrates abundant colocalisation of SCAMP5 and IFNsp-mVenus within the Golgi (figure 3C and online supplemental video 7). Moreover, IFNsp-mVenus, SCAMP5 and the clathrin light chain could be observed within the same vesicle (figure 3D). As clathrin is involved in both endocytic and exocytic pathways,¹⁸ we hypothesised that SCAMP5 is an integral component of the trafficking machinery in cells in which it is expressed and is positioned to participate in IFN-I secretion mechanisms.

Quantitative expression analysis on SCAMP5 in pDCs from genotyped donors and assays of pDC IFN-I output

We next sought to investigate the effect SCAMP5 genotypes may have on SCAMP5 expression in pDCs and to determine a potential impact on pDC function. To this end, we obtained fresh blood from homozygous carriers of the risk haplotype and non-risk haplotype tagged by rs2289583 from the Genotype

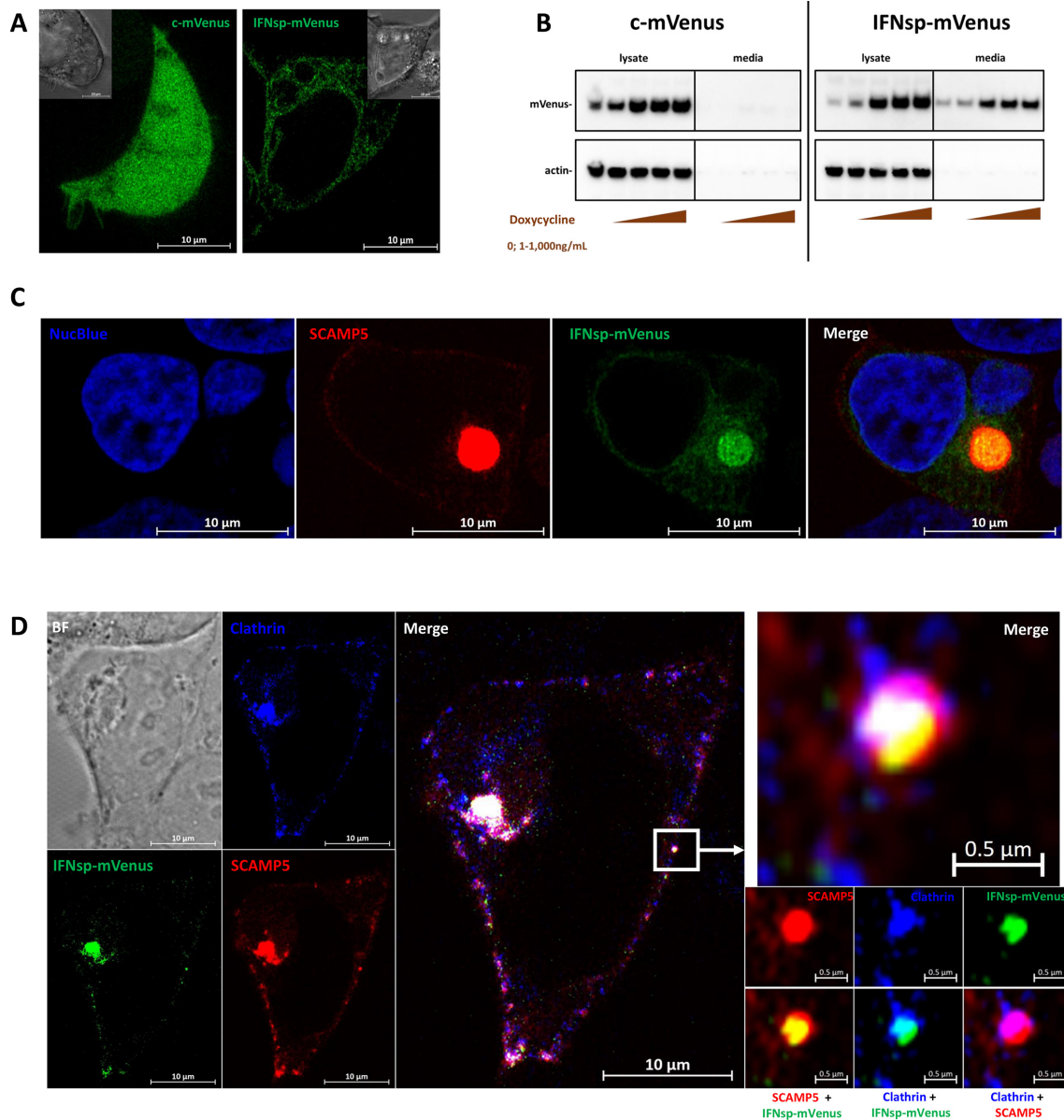


Figure 3 SCAMP5 co-traffic with the IFN- α secretory pathway. Soluble c-mVenus and IFNsp-mVenus were transduced into HEK cells under the regulation of a Tet-On system. (A) Induction using doxycycline revealed that c-mVenus was diffusely expressed in the cytoplasm, whereas IFNsp-mVenus exhibited a lacy pattern characteristic of the ER. Insets represent brightfield images. (B) c-mVenus and IFNsp-mVenus were expressed in a doxycycline dose-responsive manner as determined by western blotting using an anti-GFP antibody. c-mVenus was restricted to intracellular expression, whereas IFNsp-mVenus was detected in cell lysates as well as the culture media. (C) Coexpression of IFNsp-mVenus and SCAMP5-mKate2 reveals colocalisation of SCAMP5 with the IFN- α secretory pathway. (D) SCAMP5 colocalises with IFNsp-mVenus and clathrin in the Golgi apparatus as well as in the vesicles on the cell surface. Magnification of a single vesicle (white box) reveals SCAMP5 and clathrin coating the surface of the vesicle, with IFNsp-mVenus occupying the lumen. (A and C) 63 \times with oil immersion; (D) 100 \times with oil immersion. NucBlue delineates the nucleus. See online supplemental material for fluorescent protein designs. Correlate with online supplemental video 5, online supplemental video 6, online supplemental video 7. BF, brightfield; ER, endoplasmic reticulum; GFP, green-fluorescent protein; HEK, human embryonic kidney; IFN, interferon.

and Phenotype Registry, a resource previously used in genotype-phenotype investigations in autoimmune disease (online supplemental tables S1 and S2).^{19–21}

For expression quantitative trait locus (eQTL) analysis, quantitative RT-PCR for *SCAMP5* and the neighbouring genes, *CSK*, *COX5A*, *RPP25* and *PPCDC*, was performed. No significant differences in mRNA levels were seen for *SCAMP5*, *COX5A*, *RPP25* or *PPCDC*

(figure 4A and online supplemental figure S3). Nominal evidence of an eQTL effect was observed for *CSK*, with elevated *CSK* transcript in the risk haplotype when normalised to 18s rRNA or *IRF7* (online supplemental figure S3). To explore whether the risk haplotype polymorphisms might exert their effect at the level of translation, SCAMP5 protein was measured in pDC lysates. Median SCAMP5 protein levels were

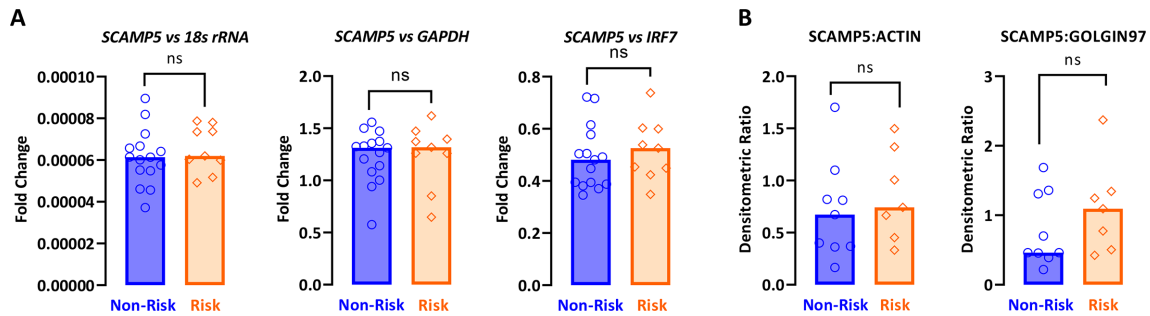


Figure 4 Comparative *SCAMP5* expression in pDCs from donors homozygous for the risk or non-risk haplotypes about rs2289583. (A) Quantitative RT-PCR for *SCAMP5* transcript from pDCs normalised individually to a highly expressed housekeeping gene (18s rRNA), a moderately expressed housekeeping gene (*GAPDH*) and a pDC-specific housekeeping gene (*IRF7*, to account for small differences in pDC purity). (B) Quantitative determination of *SCAMP5* protein-level expression by western blotting normalising individually to either actin or golgin-97. Comparisons between genotypes by Mann-Whitney test. ns, not significant; pDCs, plasmacytoid dendritic cells; RT-PCR, reverse transcription PCR.

increased in the risk haplotype when normalised to golgin-97; however, this observation was not statistically significant (figure 4B).

As some risk variants only manifest endophenotypic effects upon cell stimulation (response eQTL, reQTL),²² we next assessed for a phenotypic difference between genotypes at the functional level. Culture media from pDCs stimulated with influenza H1N1, imiquimod or ODN-2216 for 4 and 24 hours were assayed for pan-subtype IFN- α . When comparing total results from donors for either haplotype, IFN output trended towards lower values for pDCs from the risk group (figure 5A). This difference reached statistical significance only for influenza virus stimulation at the earlier time point.

To determine whether the expression of *SCAMP5* in pDCs was influenced by stimulation with influenza

virus in a genotype-dependent manner, potentially explaining the kinetic differences in IFN- α production seen above, we assayed for *SCAMP5* expression and observed that *SCAMP5* is downregulated on stimulation with influenza virus by 4 hours, with no significant differences by genotype (figure 5B). Moreover, there were no consistent differences in IFN- α transcript induction in this condition between the genotypes (figure 5B).

Taken together, these findings suggest, but do not prove, that the *SCAMP5* risk haplotype may be related to a delay in IFN protein production or secretion in the early period after viral infection.

Identification of novel *SCAMP5* splice variants in pDCs

To address the possibility that the *SCAMP5* risk haplotype influences pDC-specific *SCAMP5* isoform expression not

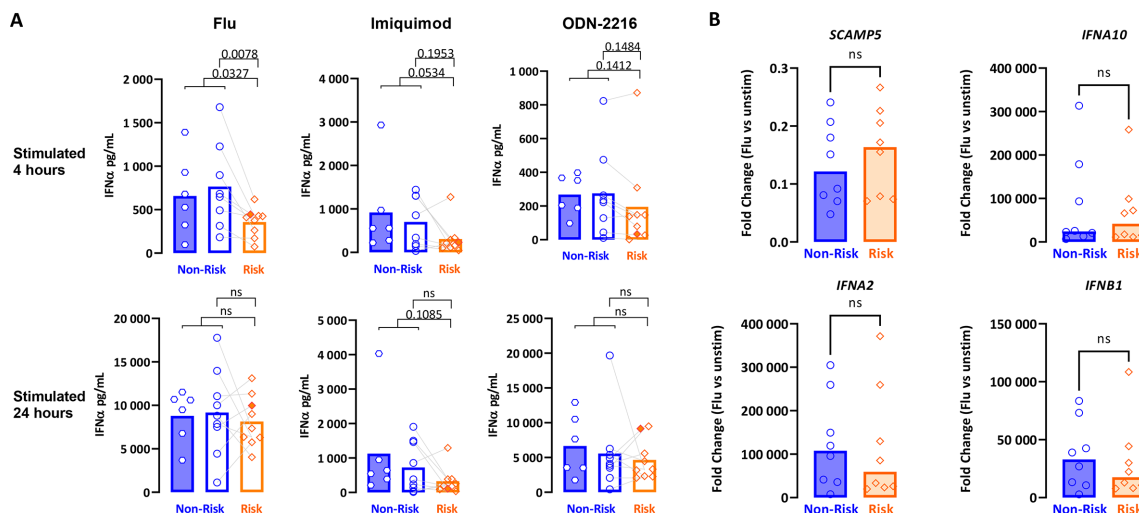


Figure 5 Comparative regulation of IFN- α and *SCAMP5* in pDCs from donors homozygous for the risk or non-risk haplotypes about rs2289583 in response to various stimuli. (A) Isolated pDCs were stimulated individually using influenza virus H1N1, imiquimod or ODN-2216 for 4 and 24 hours on separate stimulation plates per time point. Culture media were assayed for IFN- α using a pan-subtype ELISA. Each data point represents biological triplicates of 3000 pDCs per condition. Lines connect paired non-risk/risk pDCs collected and assayed on the same day. (B) Quantitative RT-PCR for *SCAMP5*, *IFNA2*, *IFNA10* and *IFNB1* from pDCs cultured for 4 hours with influenza H1N1. Data were normalised to *GUSB* expression and compared with paired samples from unstimulated (unstim) wells at 4 hours by the $\Delta\Delta C_t$ method. IFN, interferon; ns, not significant; pDCs, plasmacytoid dendritic cells; RT-PCR, reverse transcription PCR.

detected by our PCR and protein assays, we recalled an additional four risk donors and five non-risk donors for pDC isolation towards total RNAseq and de novo characterisation of *SCAMP5* splice variants. Our data reveal the existence of three novel, intron-retaining *SCAMP5* isoforms (online supplemental figure S4). These isoforms were not detected in the human neuroblastoma cell line SH-SY5Y, suggesting pDC-specific expression of these isoforms. Nonetheless, expression of these isoforms did not differ by genotype when specific primers were used for their quantification by quantitative RT-PCR.

DISCUSSION

We have investigated a novel candidate SLE risk gene, *SCAMP5*, located on chromosome 15q24. An intronic variant in *CSK*, ~155 kb distant from *SCAMP5*, was previously reported to be associated with SLE by our group and others.^{11 16} However, as shown in figure 1, a more detailed analysis of this region in a larger data set has suggested the presence of an independent genetic effect located within the *SCAMP5* gene.

SCAMP5 is a member of the SCAMP gene family and is specifically expressed in neuronal cells of the central nervous system. Interestingly, *SCAMP5* is present in the neurohypophysis, derived from neuroectoderm, and is absent in the adenohypophysis, derived from Rathke's pouch, implying tight ontogenic control over *SCAMP5* expression.¹³ In cells of the immune system, we found that *SCAMP5* is uniquely and highly expressed in pDCs, a rare cell type with the capacity to produce large amounts of IFN-I. Given the importance of IFN-I in SLE, and the large body of literature attributing pDCs as a major source of IFN-I in SLE, we pursued further analysis of *SCAMP5* function in pDCs.

SCAMP5 is highly conserved. Rare copy number variations in *SCAMP5* can lead to severe neurological phenotypes in humans and mice, while coding-level variants in *SCAMP5* are extremely rare.^{23–26} Therefore, we expected that a pDC-specific regulatory variant acting in pDCs underlies the association with SLE. In neuronal cells, the SCAMP family of proteins has been implicated in various roles in intracellular vesicular trafficking, including cargo sorting, endocytosis and exocytosis.²⁷ *SCAMP5* was shown to be necessary for the sustained release of neurotransmitter-preloaded synaptic vesicles in response to tonic stimulation. In the absence of *SCAMP5*, membrane recycling pathways were disrupted, leading to the depletion of the synaptic vesicle reserve pool and neurons refractory to further stimulation.²⁸ Elsewhere, *SCAMP5* has been reported to facilitate the export of signal-peptide containing cytokines, whereas cytokines exported via Golgi-independent pathways were unaffected by *SCAMP5* expression.²⁹ Taken together, a highly specialised role for *SCAMP5* in protein trafficking/membrane recycling seems likely.

pDCs are noteworthy for their capacity to secrete tremendous amounts of protein, including all members

of the IFN-I family (with the exception of IFN- κ). This undoubtedly requires efficient mechanisms for protein packaging and subsequent export. IFN-I is secreted along the classical pathway: a signal sequence directs nascent polypeptide chains to the ER, where the protein is translated directly into the ER lumen. Proteins destined for export are then transported to the Golgi apparatus, where sequential protein processing and sorting take place en route to the cell surface via protein-loaded vesicles.³⁰ Using IFN α -mVenus as a traceable surrogate for IFN-I secretion, we have observed that the signal peptide from IFN- α indeed directs protein synthesis to the ER, with later presence in the Golgi. We have also observed that *SCAMP5* localises predominantly to the Golgi, with puncta present on the cell surface which traffic to the Golgi in a bidirectional fashion. With these observations, we hypothesised that *SCAMP5* licenses the hypersecretory capacity of pDCs by continuous replenishment of Golgi membrane lost to exocytosis on the cell surface. While it stands to reason that any protein destined for secretion via the Golgi may be affected by this process, we focused on IFN- α secondary to its association with SLE and its relative abundance versus other pDC-derived cytokines.

To test our hypotheses, we isolated pDCs to high purity from female donors of childbearing age homozygous for risk or non-risk haplotypes about rs2289583. pDCs from these donors were used in expression-level and functional assays. *SCAMP5* expression was similar between the genotypes in unperturbed pDCs, ruling out a baseline eQTL. At the protein level, *SCAMP5* had a median higher expression in the risk group when normalised to a Golgi membrane protein loading control; however, the magnitude of this difference and the limited number of samples precluded statistical significance. The possibility that *SCAMP5* is differentially regulated between the genotypes upon stimulation was not supported by our reQTL analysis. Finally, whether a novel *SCAMP5* isoform exists in pDCs and explains the association with SLE was explored using RNAseq. Novel putative isoforms of *SCAMP5* in pDCs were detected; however, they did not differ in expression levels between the genotypes.

The expression of neighbouring genes to either side of *SCAMP5* was likewise similar, with the exception of *CSK*, which exhibits a minor (<1.2-fold) yet statistically significant increase in expression in the risk group. This may reflect the small residual LD between rs2289583 and the previously identified independent *CSK* risk haplotype, which has been associated with increased *CSK* expression in B cells. However, we note that *CSK* expression in pDCs is low in comparison with B cells. Thus, to the extent that we can identify pDC phenotypes regulated by rs2289583, *SCAMP5* remained a leading candidate gene to explore.

Functionally, pDCs from risk donors produce less IFN- α on average compared with non-risk, when stimulated with imiquimod, ODN-2216 or influenza virus at 4 or 24 hours of stimulation. These differences were more pronounced with imiquimod and influenza virus—both TLR7 agonists—and at the earlier time point. These data

run counter to the expectation that SLE risk variants in the IFN pathway *increase* IFN production. With the exception of SLE variants in *STAT4* which increase sensitivity to signalling through the IFN- α/β receptor, resulting in decreased serum IFN activity,³¹ most IFN-related SLE risk variants indeed confer a greater predilection for IFN production.³² Statistically significant differences in these studies usually involve dozens or hundreds of representatives of each genotype, and IFN presence is often inferred through biological activity assays rather than direct IFN measurements as performed here.

Our observations raise several possibilities. The IFN production defect is more pronounced at 4 hours than at 24 hours, suggesting that a kinetic trait in IFN export may be at play. Rapid production of IFN is critical for antiviral defence. As viral prodromes often precede onset of SLE symptoms, it may be the case that enhanced susceptibility to viral infection through slower IFN secretion may induce SLE in an otherwise susceptible host. Alternatively, the observed IFN secretion defect may represent an incidental finding unrelated to SCAMP5's role in pDCs. That SCAMP5 colocalises with the IFN- α secretory pathway does not necessarily indicate an interaction between the two. CRISPR knockout studies in primary pDCs may be necessary for establishing a definitive link between SCAMP5 and IFN secretion. We have successfully used CRISPR to knock out BDCA4 expression in primary human pDCs (online supplemental figure S5); however, knockout of SCAMP5 has proven elusive, possibly due to longer half-life of this protein in these short-lived cells.

Separately, we have investigated human pDC responses to influenza virus by secretome profiling using liquid chromatography tandem mass spectrometry and at the single pDC level using single cell RNAseq (Ghanem MH *et al*, 2021, manuscript in preparation). There, we observed that *SCAMP5* is widely expressed in pDCs immediately *ex vivo*, but is downregulated upon stimulation, implying a role of SCAMP5 that is distinct from ongoing IFN export. Moreover, we observed evidence for granzyme B release from these cells via a mechanism consistent with degranulation rather than the classic secretory pathway. A role of SCAMP5 in this process would bear more similarity to synaptic vesicle release from neuronal cells where the function of SCAMP5 is more thoroughly described. These possibilities are being addressed by ongoing investigation. This work marks the first description of a role of SCAMP5 in pDC biology and IFN secretion; much remains to be explored.

Acknowledgements We would like to acknowledge the participants of the GaP Registry for their contribution to this work. Gila Klein, Margaret DeFranco, Kristine Elmaliki and Dorean Flores coordinated GaP donor recall and sample collections. Professor Timothy Vyse (King's College London) kindly provided primary SNP data on SLE cases and controls. Christopher Colon, Heriberto Borrero and Barrett Waling provided assistance with flow cytometry. Amanda Chan and Anita Ng provided assistance with confocal microscopy. Anthony Liew performed the library construction and sequencing for total RNAseq. We thank Professor David Castle (University of Virginia) for helpful discussions on SCAMP5. Lentiviral constructs were cloned using vectors provided by Addgene.

Contributors MHG, SJK, KRS and PKG conceived and designed the study. MHG, HV and LNC collected the experimental data. MHG and KRS analysed the experimental data. AS performed the RNAseq analysis. WL performed the statistical genetics analysis. MHG, KRS and PKG wrote the manuscript. PKG was the principal investigator on the study and serves as the guarantor of this work. All authors revised and approved the final manuscript.

Funding This work is supported by a career development award to KRS (NIH K01AR071502) and awards to SJK (R01 AR075565 and U19 AI144306), as well as departmental funds provided by the Center for Genomics and Human Genetics at the Feinstein Institutes for Medical Research.

Competing interests None declared.

Patient consent for publication Not required.

Ethics approval The Genotype and Phenotype (GaP) Registry at the Feinstein Institutes for Medical Research provided de-identified blood from donors consented under an IRB-approved protocol (IRB# 09-081). The Committee for Participant Protection at the Feinstein Institutes for Medical Research approved this study (TAPO307.5.73). The GaP is a subprotocol of the Tissue Donation Program (TDP) at Northwell Health and a national resource for genotype-phenotype studies (<https://www.feinsteininstitute.org/robert-sboas-center-for-genomics-and-human-genetics/gap-registry/>).

Provenance and peer review Not commissioned; externally peer reviewed.

Data availability statement Data are available in a public, open access repository. Data are available upon reasonable request. RNA-seq data will be uploaded to GEO and may also be directly available through our group.

Supplemental material This content has been supplied by the author(s). It has not been vetted by BMJ Publishing Group Limited (BMJ) and may not have been peer-reviewed. Any opinions or recommendations discussed are solely those of the author(s) and are not endorsed by BMJ. BMJ disclaims all liability and responsibility arising from any reliance placed on the content. Where the content includes any translated material, BMJ does not warrant the accuracy and reliability of the translations (including but not limited to local regulations, clinical guidelines, terminology, drug names and drug dosages), and is not responsible for any error and/or omissions arising from translation and adaptation or otherwise.

Open access This is an open access article distributed in accordance with the Creative Commons Attribution Non Commercial (CC BY-NC 4.0) license, which permits others to distribute, remix, adapt, build upon this work non-commercially, and license their derivative works on different terms, provided the original work is properly cited, appropriate credit is given, any changes made indicated, and the use is non-commercial. See: <http://creativecommons.org/licenses/by-nc/4.0/>.

ORCID iDs

Mustafa H Ghanem <http://orcid.org/0000-0002-8019-5324>

Andrew J Shih <http://orcid.org/0000-0001-8375-7313>

Himanshu Vashistha <http://orcid.org/0000-0003-4653-5011>

Latanya N Coke <http://orcid.org/0000-0001-9018-0188>

Wentian Li <http://orcid.org/0000-0003-1155-110X>

Sun Jung Kim <http://orcid.org/0000-0001-8535-5537>

Kim R Simpfendorfer <http://orcid.org/0000-0002-1906-2899>

Peter K Gregersen <http://orcid.org/0000-0003-1613-1518>

REFERENCES

- 1 Reizis B. Plasmacytoid dendritic cells: development, regulation, and function. *Immunity* 2019;50:37–50.
- 2 Baechler EC, Batliwalla FM, Karypis G, *et al*. Interferon-Inducible gene expression signature in peripheral blood cells of patients with severe lupus. *Proc Natl Acad Sci U S A* 2003;100:2610–5.
- 3 Vermi W, Lonardi S, Morassi M, *et al*. Cutaneous distribution of plasmacytoid dendritic cells in lupus erythematosus. Selective tropism at the site of epithelial apoptotic damage. *Immunobiology* 2009;214:877–86.
- 4 Arazi A, Rao DA, Berthier CC, *et al*. The immune cell landscape in kidneys of patients with lupus nephritis. *Nat Immunol* 2019;20:902–14.
- 5 Furie R, Werth VP, Merola JF, *et al*. Monoclonal antibody targeting BDCA2 ameliorates skin lesions in systemic lupus erythematosus. *J Clin Invest* 2019;129:1359–71.
- 6 Sisirak V, Ganguly D, Lewis KL, *et al*. Genetic evidence for the role of plasmacytoid dendritic cells in systemic lupus erythematosus. *J Exp Med* 2014;211:1969–76.

- 7 Son M, Kim SJ, Diamond B. SLE-associated risk factors affect DC function. *Immunol Rev* 2016;269:100–17.
- 8 Jego G, Palucka AK, Blanck J-P, et al. Plasmacytoid dendritic cells induce plasma cell differentiation through type I interferon and interleukin 6. *Immunity* 2003;19:225–34.
- 9 Soni C, Perez OA, Voss WN, et al. Plasmacytoid dendritic cells and type I interferon promote extrafollicular B cell responses to extracellular Self-DNA. *Immunity* 2020;52:1022–38.
- 10 Crow MK, Olfert M, Kirou KA. Type I interferons in autoimmune disease. *Annu Rev Pathol* 2019;14:369–93.
- 11 Bentham J, Morris DL, Graham DSC, et al. Genetic association analyses implicate aberrant regulation of innate and adaptive immunity genes in the pathogenesis of systemic lupus erythematosus. *Nat Genet* 2015;47:1457–64.
- 12 Hubbard C, Singleton D, Rauch M, et al. The secretory carrier membrane protein family: structure and membrane topology. *Mol Biol Cell* 2000;11:2933–47.
- 13 Fernández-Chacón R, Südhof TC. Novel SCAMPs lacking NPF repeats: ubiquitous and synaptic vesicle-specific forms implicate SCAMPs in multiple membrane-trafficking functions. *J Neurosci* 2000;20:7941–50.
- 14 Uhlén M, Fagerberg L, Hallström BM, et al. Proteomics. Tissue-based map of the human proteome. *Science* 2015;347:1260419.
- 15 Hom G, Graham RR, Modrek B, et al. Association of Systemic Lupus Erythematosus with *C8orf13-BLK* and *ITGAM-ITGAX*. *N Engl J Med Overseas Ed* 2008;358:900–9.
- 16 Manjarrez-Orduño N, Marasco E, Chung SA, et al. Csk regulatory polymorphism is associated with systemic lupus erythematosus and influences B-cell signaling and activation. *Nat Genet* 2012;44:1227–30.
- 17 Su AI, Cooke MP, Ching KA, et al. Large-Scale analysis of the human and mouse transcriptomes. *Proc Natl Acad Sci U S A* 2002;99:4465–70.
- 18 Brodsky FM. Diversity of clathrin function: new tricks for an old protein. *Annu Rev Cell Dev Biol* 2012;28:309–36.
- 19 Simpfordorfer KR, Armstead BE, Shih A, et al. Autoimmune disease-associated haplotypes of *blk* exhibit lowered thresholds for B cell activation and expansion of Ig class-switched B cells. *Arthritis Rheumatol* 2015;67:2866–76.
- 20 Li D, Matta B, Song S, et al. IRF5 genetic risk variants drive myeloid-specific IRF5 hyperactivation and presymptomatic SLE. *JCI Insight* 2020;5. doi:10.1172/jci.insight.124020. [Epub ahead of print: 30 Jan 2020].
- 21 Gregersen PK, Klein G, Keogh M, et al. The genotype and phenotype (GAP) registry: a living Biobank for the analysis of quantitative traits. *Immunol Res* 2015;63:107–12.
- 22 Kim-Hellmuth S, Bechheim M, Pütz B, et al. Genetic regulatory effects modified by immune activation contribute to autoimmune disease associations. *Nat Commun* 2017;8:266.
- 23 Castermans D, Volders K, Crepel A, et al. SCAMP5, NBEA and AMISYN: three candidate genes for autism involved in secretion of large dense-core vesicles. *Hum Mol Genet* 2010;19:1368–78.
- 24 Hubert L, Cannata Serio M, Villoing-Gaudé L, et al. De novo SCAMP5 mutation causes a neurodevelopmental disorder with autistic features and seizures. *J Med Genet* 2020;57:138–44.
- 25 Zhang D, Yuan C, Liu M, et al. Deficiency of SCAMP5 leads to pediatric epilepsy and dysregulation of neurotransmitter release in the brain. *Hum Genet* 2020;139:545–55.
- 26 Dickinson ME, Flenniken AM, Ji X, et al. High-throughput discovery of novel developmental phenotypes. *Nature* 2016;537:508–14.
- 27 Law AHY, Chow C-M, Jiang L. Secretory carrier membrane proteins. *Protoplasma* 2012;249:269–83.
- 28 Park D, Lee U, Cho E, et al. Impairment of release site clearance within the active zone by reduced SCAMP5 expression causes short-term depression of synaptic release. *Cell Rep* 2018;22:3339–50.
- 29 Han C, Chen T, Yang M, et al. Human SCAMP5, a novel secretory carrier membrane protein, facilitates calcium-triggered cytokine secretion by interaction with SNARE machinery. *J Immunol* 2009;182:2986–96.
- 30 Lacy P, Stow JL. Cytokine release from innate immune cells: association with diverse membrane trafficking pathways. *Blood* 2011;118:9–18.
- 31 Kariuki SN, Kirou KA, MacDermott EJ, et al. Cutting edge: autoimmune disease risk variant of STAT4 confers increased sensitivity to IFN-alpha in lupus patients in vivo. *J Immunol* 2009;182:34–8.
- 32 Ghodke-Puranik Y, Niewold TB. Genetics of the type I interferon pathway in systemic lupus erythematosus. *Int J Clin Rheumatol* 2013;8:657–69.

Supplementary materials for:

Investigations into *SCAMP5*, a candidate lupus risk gene expressed in plasmacytoid dendritic cells

By Ghanem et al.

Materials and Methods

Human blood donors

The Genotype and Phenotype (GaP) Registry at The Feinstein Institutes for Medical Research provided de-identified blood from donors consented under an IRB-approved protocol (IRB# 09-081). The Committee for Participant Protection at The Feinstein Institutes for Medical Research approved this study (TAP0307.5.73). The GaP is a sub-protocol of the Tissue Donation Program (TDP) at Northwell Health and a national resource for genotype-phenotype studies (<https://www.feinsteininstitute.org/robert-sboas-center-for-genomics-and-human-genetics/gap-registry/>). For experiments comparing genotypes, subjects were selected on the basis of genotype from the Global Screening Array (GSA).

Patient and Public Involvement

Patients in our studies are actively interested in advancing knowledge of autoimmunity, even when they participate as controls in protocols such as the GaP. Thus, a Community Advisory Board comprised of diverse (ethnicity, age and gender) community members and study participants are consulted quarterly, and their input is integrated into the GaP study. Patients have not been involved in the design of the experimental work. There were no interventions in this study. The results will be communicated via publication and newsletters to participants.

FACS analysis and cell sorting

Fresh whole blood was drawn from healthy donors into sodium-heparin vacutainers (BD). PBMCs were extracted over Ficoll-Paque (GE Healthcare) using standard methods. PBMCs were then labeled as follows for cell sorting: CD19, CD3, CD4, CD8, CD56, CD14, CD16, CD304, CD303, CD11c, HLA-DR. Lymphocytes were sorted by gating on the lymphocyte population on light scatter: B cells (CD19+CD3-CD56-); CD4 T cells (CD3+CD4+); CD8 T cells (CD3+CD8+); NK cells (CD56+CD3-CD19-). Monocytes were sorted by gating on the monocyte population on light scatter: CD14 classical monocytes (CD14+CD16-); CD16 non-classical monocytes (CD16+CD14-). Dendritic cells were sorted by gating on the lineage negative population (CD19-CD3-CD56-CD16-): pDCs (CD304+CD303+); cDCs (HLA-DR+CD11c+). Cells were sorted into microfuge tubes on the BD FACSAria SORP cell sorter. Sorted cells were immediately pelleted by centrifugation and frozen dry at -80°C until RNA extraction for RT-PCR or lysate preparation for western blotting.

For intracellular staining of SCAMP5 and flow cytometric analysis, PBMCs were surface stained for CD304 (BDCA-4) followed by fixation and permeabilization using BD Cytofix/CytoPerm. Cells were then kept in BD Perm/Wash and stained for SCAMP5 using a rabbit polyclonal antibody (PA5-61269, ThermoFisher Scientific) followed by staining using anti-rabbit AF488. Cells were acquired using the BD Fortessa flow cytometer.

mRNA Expression

RNA was prepared from frozen cell pellets using the Qiagen RNeasy Micro Plus kit (Qiagen 74034). RNA was immediately reverse transcribed using Superscript IV VILO master mix at 50°C for 10 minutes (Invitrogen 11756050), or the SuperScript IV VILO Master Mix 'No RT' Control, using the Applied Biosystems Veriti thermal cycler. cDNA was then diluted in TE buffer and stored at -20°C pending further analysis. qPCR was performed using Taqman assays (ThermoFisher Scientific) and Taqman Gene Expression Master Mix (Applied Biosystems 4369016). qPCR reactions were performed on the Applied Biosystems Vii7 thermal cycler.

Protein expression studies

Lysates were prepared by resuspending cell pellets in 1X CHAPS lysis buffer supplemented with 1X HALT protease inhibitor (Thermo Scientific 78429). Lysates were incubated on ice for 30 minutes with periodic vortexing. LDS sample buffer was added to a final concentration of 1X and β -mercaptoethanol to a final concentration of 5%. Lysates were then directly loaded into a 10% Bis-Tris gel without boiling, as heating of lysates was found to aggregate SCAMP5 protein. Lysates were resolved at 200V for 45 minutes using 1X Novex BOLT running buffer. Gels were then equilibrated in 1X Novex Transfer buffer/20% methanol, followed by transfer onto 0.45 μ M PVDF membranes at 100V/350mA for 25 minutes. Blots were blocked for 60 minutes at room temperature using Licor Odyssey Blocking Buffer diluted 1:1 in PBS. Primary anti-SCAMP5 rabbit polyclonal antibody (PA5-61269) was diluted in staining buffer (Licor blocking buffer diluted 1:5 in PBS) at a dilution of 1:1,000 overnight at 4°C. After 3 washes in PBS Tween-20, secondary anti-rabbit HRP was added at a dilution of 1:10,000 in staining buffer for 2 hours at room temperature. After another 2 rounds of washing in PBS-T and a final wash in PBS, the blot was developed using chemiluminescent substrate and acquired using the BioRad Chemidoc Imager. The blot was reprobbed for actin (Ab clone AC-15) as described for SCAMP5.

Confocal microscopy of pDCs

For confocal analysis of SCAMP5 in pDCs, pDCs were isolated from PBMCs by immunomagnetic negative selection. Freshly isolated pDCs were cytospun onto charged glass slides. Cells were fixed and permeabilized by immersion in BD Cytfix/Cytoperm, and simultaneously stained for SCAMP5 (rabbit polyclonal antibody PA5-61269) and Golgin-97 (ThermoFisher A-21270). A pre-immune rabbit polyclonal antibody was used as a negative control for SCAMP5 staining, (no staining was observed, data not shown). Cells were washed in BD Perm/Wash and stained using anti-rabbit AF488 and anti-mouse AF647. No. 1 coverslips were mounted using Prolong Antifade Glass with NucBlue and sealed using clear nail polish. After curing at 4°C for 30 minutes, images were acquired using the Zeiss LSM 880 confocal microscope.

Genomic analysis of the SLE association polymorphism rs2289583

Phased haplotypes were built from genotypes of rs2472300, rs6495122 and rs2289583 for 6,959 controls and 4,036 lupus cases (totaling 10,995 subjects and 21,990 haplotypes). Plink binary files were converted to a vcf file with plink2. Variants were phased using beagle 5.0 (v2018) using the hg37 genetic map. P values and odds ratios were calculated by comparing counts of each haplotype to the sum of other haplotypes.

Linkage disequilibrium (LD) statistics between SNPs were obtained using the 'LDpair Tool' on LD Link (<https://ldlink.nci.nih.gov/?tab=ldpair>) (Machiela and Chanock, 2015). LD statistics were derived from the European population.

Conditional analysis was carried out by multi-variable logistic regression, with the SNP to be conditioned as one of the independent variables, and phenotype being the dependent variable. The coefficients and the corresponding p-values for other SNPs, being other independent variables, are the association results conditional on the SNP to be conditioned.

Phenotyping of GaP Subjects on the basis of *SCAMP5* risk haplotype

The GaP Registry is a cohort of ~7,500 (and counting) genotyped healthy individuals who have agreed to recall on the basis of their genotype.¹⁹ The GaP has been previously utilized for the study of endophenotypes regulated by various autoimmune risk variants and is available to the scientific community.^{16 20 21} To assay for pDC phenotypes related to genotype at rs2289583, we chose from among this cohort. As the relationship of the causal polymorphism to rs2289583 has not yet been established, we sought to enrich for likely carriers of the causal allele by constructing SLE risk haplotypes inclusive of rs2289583. rs6495122 and rs2472300 are the next most significantly associated SNPs in the region and together along with rs2289583 they denote a risk haplotype.

Female subjects of childbearing age (here stipulated 18-40) homozygous for the risk or non-risk haplotypes were contacted for recall (subject characteristics in **Table S2**). 60CC whole blood was drawn from each donor into sodium-heparin vacutainers. Subjects were drawn in pairs, with one homozygous risk and one homozygous non-risk donor per day. Altogether, 9 risk:non-risk pairs were collected, with an additional 3 non-risk:non-risk pairs, over 12 discontinuous days of sampling.

Whole blood lysates were genotyped to confirm the fidelity of the recalled subject genotypes. Taqman genotyping was performed for rs2289583 on crude whole blood lysates: Frozen aliquots of whole blood were thawed and prepared for PCR using DNA Extract All Reagents Kit (Applied Biosystems 4403319). PCR was performed using a custom Taqman genotyping assay (assay ID: C__15881999_10) and TaqPath ProAMP Master Mix (Applied Biosystems A30865), with the VIC probe detecting the minor allele (A=risk) and the FAM probe detecting the major allele (C=non-risk). Genotypes were called on the Vii7 Real-Time PCR System (Applied Biosystems).

PBMCs were extracted over Ficoll-Paque using established methods. A small aliquot of PBMCs was kept for determination of baseline pDC frequency. pDCs were isolated using Miltenyi Biotec Human Plasmacytoid Dendritic Cell Isolation Kit II (130-097-415) in accordance with the manufacturer's protocol. A small aliquot of isolated pDCs was used for purity determination by staining for BDCA4 and BDCA2 (**Figure S6**).

For pDC stimulation cultures, 3,000 pDCs were cultured per well of a round-bottom 96-well plate using Advanced RPMI (Gibco 12633012) with 5% FCS. Triplicate cultures were established per condition: no stimulation, imiquimod 4µg/mL (Invivogen), ODN-2216 2µM (Invivogen), or influenza virus 0.4HAU/mL (A/PR/8/34 H1N1, Advanced Biotechnologies Inc.).

RNA preparation, cDNA synthesis, qPCR, and western blotting on pDC pellets were performed as described above. IFN- α ELISAs were performed using MABTECH 3425-1H-6 in accordance with the manufacturer's protocol. QTL and ELISA experiments were performed in a single batch after all GaP donors had been collected.

Taqmas assays for eQTL experiments are as follows:

Gene	Assay ID
<i>SCAMP5</i>	Hs01547727_m1
<i>PPCDC</i>	Hs00222418_m1
<i>RPP25</i>	Hs00706565_s1
<i>CSK</i>	Hs01062581_m1
<i>COX5A</i>	Hs00362067_m1
<i>18S rRNA</i>	Hs03003631_g1
<i>GAPDH</i>	Hs02786624_g1
<i>IRF7</i>	Hs01014809_g1
<i>POLR2A</i>	Hs00172187_m1
<i>IFNB1</i>	Hs01077958_s1
<i>IFNA2</i>	Hs00265051_s1
<i>IFNA10</i>	Hs03406429_gH
<i>GUSB</i>	Hs00939627_m1

Taqman assays for intron-inclusion transcripts were custom generated by ThermoFisher and are described in the table below:

Intron interval name	qPCR assay ID	Chromosome 15 (Hg38)	
		Start position	End position
1-1		7,499,567	74,995,966
1-2		7,499,632	74,997,233
1-3		7,499,731	75,007,587
1-4		7,500,772	75,009,890
1-5		7,500,994	75,011,657
1-6	APEPXWT	7,501,168	75,011,791
2-1		7,501,184	75,012,676
3-1	APFVTGP	7,501,312	75,016,592
4-1	APGZK2M	7,501,674	75,017,652
5-1		7,501,797	75,018,393
6-1		7,501,853	75,018,788

Design of lentiviral expression constructs

SCAMP5-mKate2, c-mVenus, IFNsp-mVenus and mTagBFP2-clathrin were ordered as gene blocks from IDT. SCAMP5-mKate2 was cloned into the lentiviral backbone vector pLJM1-eGFP (Addgene #19319) using NheI and BstBI in place of eGFP. c-mVenus and IFNsp-mVenus were first cloned into the Gateway entry vector pENTR4 using NcoI and XhoI followed by recombination into the lentiviral Gateway destination vector pLenti CMVtight Puro DEST (Addgene #26430) using LR Clonase II. A lentiviral backbone vector expressing rtTA3 was obtained separately (Addgene #26429).

Lentiviral vectors were produced by co-transfection of lentiviral backbone vectors along with a lentiviral packaging mix (Invitrogen A43237) carrying the Rev, VSV-G and Gag/Pol genes using Lipofectamine 3000 into HEK 293T cells. Lentiviral media was collected 72 hours post-transfection, cleared through 0.22µm syringe filters and stored at -80c.

Transduction of HEK-293T cells with lentiviral particles

For SCAMP5-mKate2 expression, SCAMP5-mKate2 lentiviral particles were transduced into HEK-293T cells. Cells expressing mKate2 were sorted on the BD FACSAria and maintained in culture. For c-mVenus and IFNsp-mVenus expression, the respective lentiviral particles were co-transduced with rtTA3 into HEK-293T cells previously transduced with SCAMP5-mKate2, to generate cells constitutively expressing SCAMP5-mKate2 and either mVenus or IFNsp-mVenus in a doxycycline inducible system.

Live-cell confocal microscopy

HEK-293T cells expressing the desired transgenes were seeded onto 35mm poly-D-lysine coated dishes with No. 1 coverslip center pieces. Prior to imaging, the media was aspirated and replaced with FluoroBrite DMEM Media containing 10% FBS, with or without NucBlue for counterstaining of nuclei. Images were acquired on a Zeiss LSM880 Confocal microscope.

pDC total RNAseq

pDCs were isolated from 4 homozygous risk and 5 homozygous non-risk donors as described above. Yield and purities are presented in the table below. pDC pellets were immediately stored at -80c. RNA extraction was performed using Qiagen RNeasy Micro Plus kit (Qiagen 74034). Sequencing libraries were prepared with normalized inputs using TruSeq RNA Single Indexes Set A (Illumina Cat. # 20020492). Paired end sequencing reactions were performed on the Illumina NextSeq 500 sequencer using NextSeq 500/550 High Output Kit v2.5 (150 Cycles) (Illumina Cat. #20024907). FastQC was used to insure there was no adapter contamination and reads had acceptable quality scores. Intronic retention was quantified using iREAD to the Gencode grch38 reference assembly.

Subject Genotype	pDC yield	pDC Purity
Non-risk / Risk	#	%Percent
3538	435,000	95.8
4752	61,272	67.4
5050	569,000	96.1
7406	217,000	94.1
2727	132,000	95.3
8640	567,000	96.5
8461	256,200	84.2
4855	229,000	81.2
8123	374,900	84.2

Data and Statistical Analyses

Unless otherwise indicated, raw data was tabulated in Microsoft Excel. ELISA standard curve interpolation, graph generation and statistical analyses were performed using GraphPad Prism. Flow cytometry data was analyzed using FlowJo. Confocal images were analyzed using ZenBlue. In all figures, numerical values are indicated for p-values <0.2, all other p-values denoted as *not significant*.

Fusion protein constructs**Scamp5-mKate2 protein sequence:**

MAEKVNNFPPLPKFIPLKPCFYQDFEADIPPQHLSLTKRLLYLWMLNSVTLAVNLVGLAWLIGGGGATNFGLAFLWLILFTPCSIVCWF
RPIYKAFKTDSSFSFMAFFFTFMAQLVISIIQAVGIPGWVCGWIATISFFGTNIGSAVVMLIPTVMFTVVAVFSFIALSMVHKFYRSGG
SFSKAQEEWTTGAWKNPHVQQAQAAMGAAQGAMNQPQTQYSATPNYYSNEMGGGGPGGGSVSELIKENMHMKLYMEG
TVNNHHFKCTSEGEGKPYEGTQTMRIKAVEGGPLPFAFDILATSFMYGSKTFINHTQGIPDFFKQSFPEGFTWERVTTYEDGGVLTATQ
DTSLQDGLIYNVKIRGVNFPNGPVMQKKTGLWEASTETLYPADGGLEGRADMALKLVGGGHLICNLKTTYRSKKPAKNLKMPGVYY
VDRRLERIKEADKETYVEQHEVAVARYCDLPSKLGHR

SCAMP5 sequence**GI₄ linker****mKate2 sequence****mVenus protein sequences:**

Sequence of mVenus with human IFN- α leader peptide [human codon-optimized]:

MALSFLLMAVLVLSYKISCSLGCPLVSKGEELFTGVVPILVELDGDVNGHKFSVSGEGGDATYGKLTCLKICTTGKLPVPWPTLVTTLG
YGLQCFARYPDHMKQHDFKSA MPEGYVQERTIFFKDDGNYKTRAEVKFEGLTLVNRIELKIDFKEDGNILGHKLEYNYNSHNVYITA
DKQKNGIKANFKIRHNIEDGGVQLADHYQNTPIGDGPVLLPDNHLSYQSKLSKDPNEKRDHMLLEFVTAAGITLGMDELYK

Sequence of untagged mVenus:

MVSKGEELFTGVVPILVELDGDVNGHKFSVSGEGGDATYGKLTCLKICTTGKLPVPWPTLVTTLG YGLQCFARYPDHMKQHDFKSA
MPEGYVQERTIFFKDDGNYKTRAEVKFEGLTLVNRIELKIDFKEDGNILGHKLEYNYNSHNVYITADKQKNGIKANFKIRHNIEDGGVQ
LADHYQNTPIGDGPVLLPDNHLSYQSKLSKDPNEKRDHMLLEFVTAAGITLGMDELYK

IFN- α leader peptide**mVenus****mTagBFP2-Clathrin protein sequence:**

MVSKGEELIKENMHMKLYMEGTVDNHHFKCTSEGEGKPYEGTQTMRIKVVVEGGPLPFAFDILATSFYGSKTFINHTQGIPDFFKQSF
EGFTWERVTTYEDGGVLTATQDTSLQDGLIYNVKIRGVNFTSNGPVMQKKTGLWEAFTETLYPADGGLEGRNDMALKLVGGSHLIA
NAKTTYRSKKPAKNLKMPGVYYVDYRLERIKEANNETYVEQHEVAVARYCDLPSKLGHKLNSGLRSRAQASNSAVDMADDFGFFSSE
SGAPEAAEEDPAAFLAQQESEIAGIENDEGFGAPAGSHAAPAQPPTS GAGSEDMGTTVNGDVFQEANGPADGYAAIAQADRLTQ
EPESIRKWREEQKRLQELDAASKVTEQEWREKAKKDLEWNRQSEQVEKNKINNRASEEAFVKESKEETPGTEWEKVAQLCDFNP
KSSKQCKDVSRLRSVLM SLKQTPLSR

mTagBFP2 sequence**Linker peptide****Clathrin light chain B isoform A**

Supplementary figures

Figure S1. Schematic of SCAMP5 topology. Generated using BioRender.

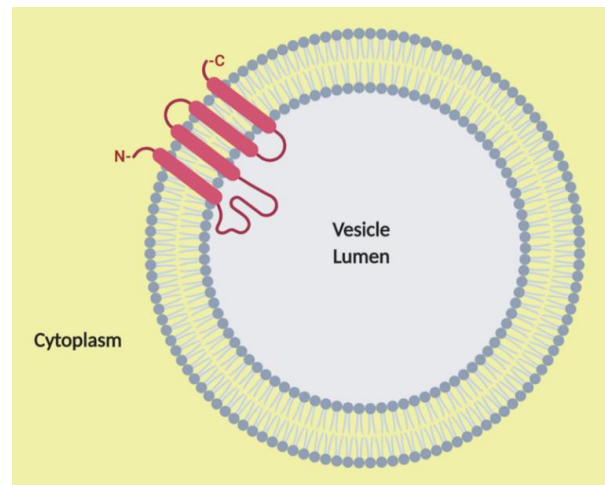


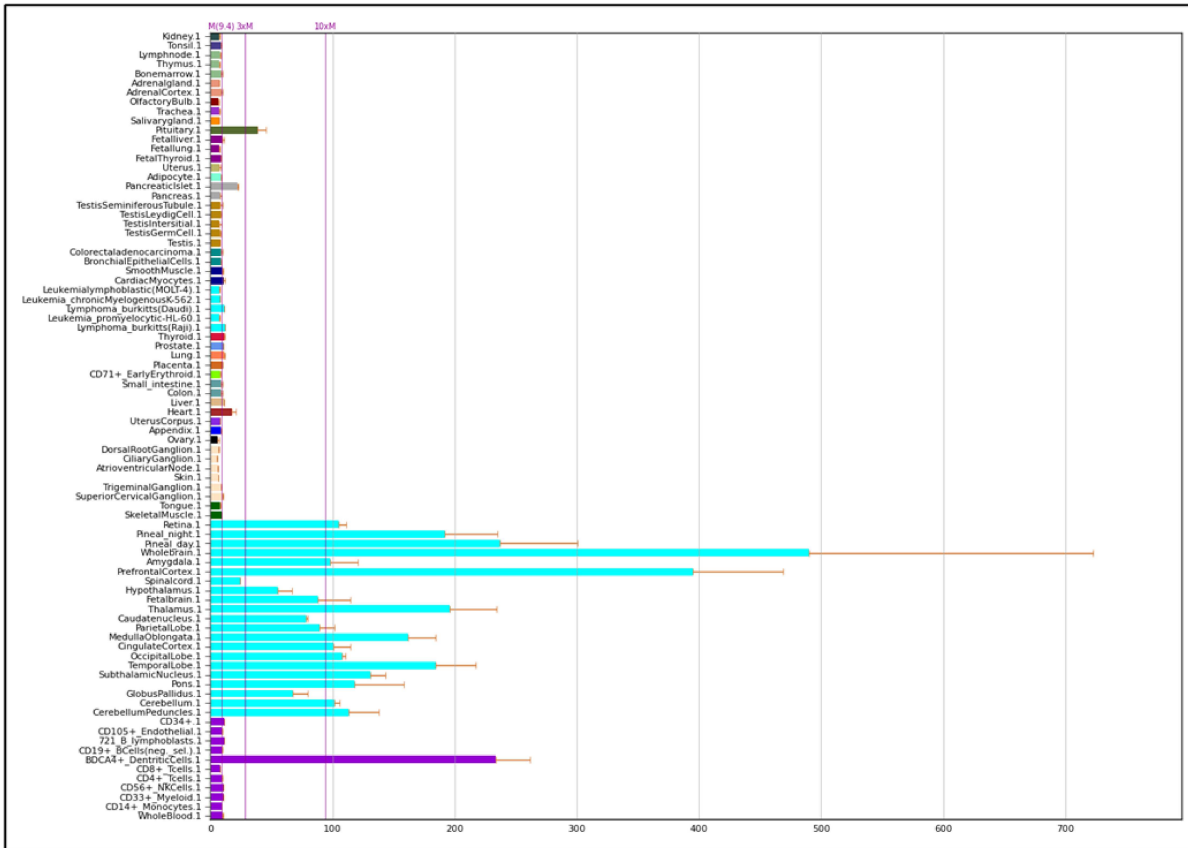
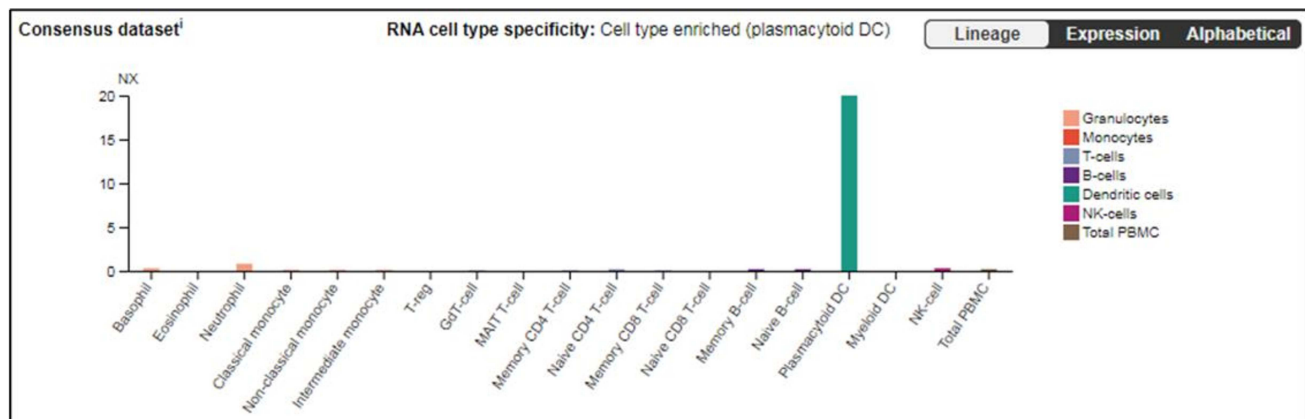
Figure S2.**A) SCAMP5 expression across human tissues determined using microarray. (BioGPS)**<http://biogps.org/#goto=genereport&id=192683>**B) SCAMP5 expression across circulating human leukocyte subsets as determined by RNA-seq. (Human Protein Atlas)**<https://www.proteinatlas.org/ENSG00000198794-SCAMP5/blood>

Figure S3. Comparative expression in pDCs of genes neighboring *SCAMP5* from donors homozygous for the risk or non-risk haplotypes about *rs2289583*. Quantitative RT-PCR for *CSK*, *COX5A*, *RPP25* and *PPCDC* transcript from pDCs normalized individually to 18s rRNA, *GAPDH* and *IRF7*. Comparisons between genotypes by Mann-Whitney test. *ns*= not significant.

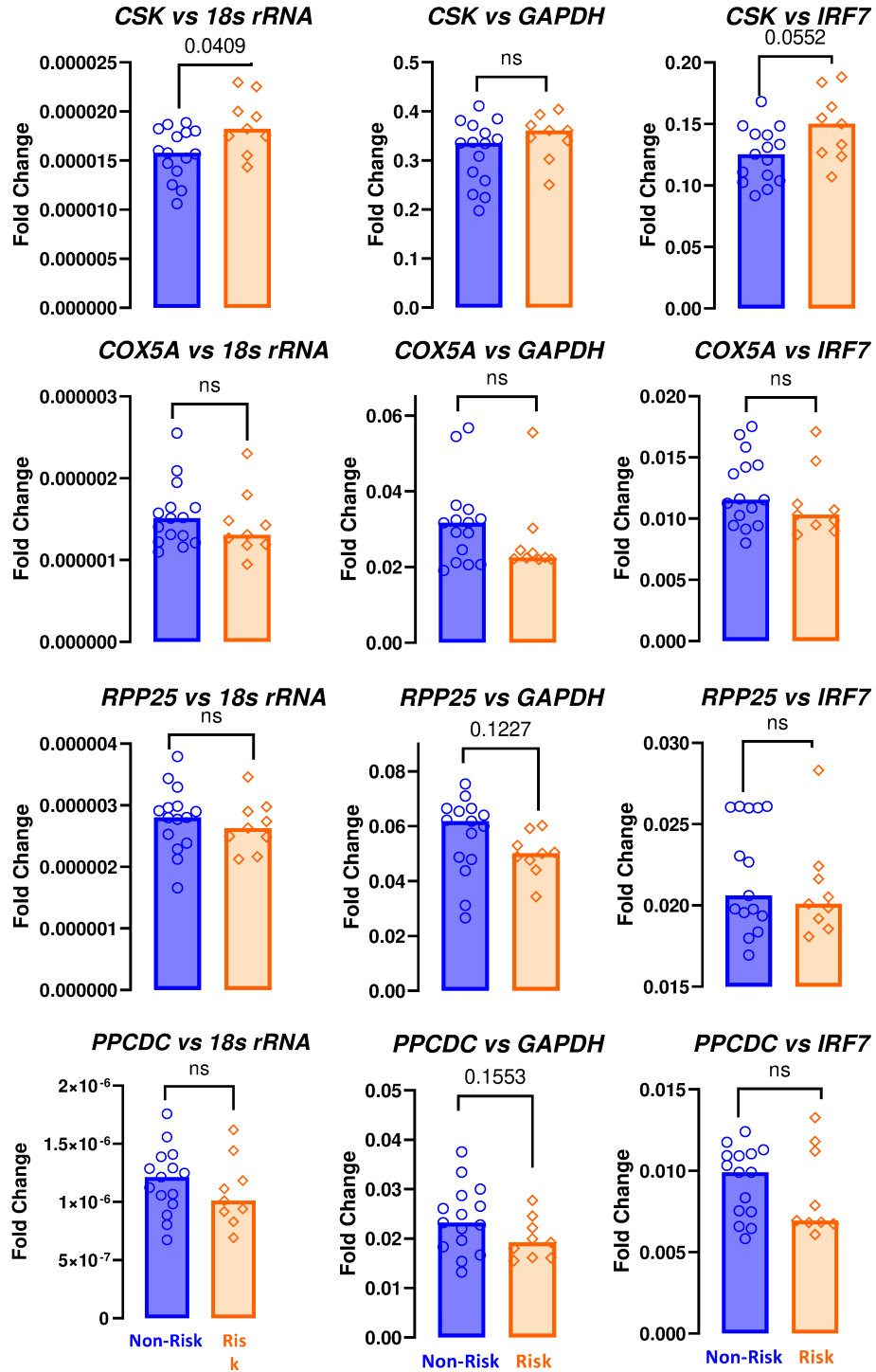


Figure S4. Expression of *SCAMP5* intron sequences. **A)** A schematic diagram of the *SCAMP5* gene (ENST00000425597) shows the location of the reported expressed intronic segments, and the identifier assigned to each. **B)** RNAseq FPKM values of *SCAMP5* intronic segments. **C)** Relative expression of the three mostly highly expressed *SCAMP5* intron segments, relative to total expression of *SCAMP5* (as measured by quantitative RT-PCR assay spanning the exon 2 to exon 3 boundaries of intron 2 of the *SCAMP5* gene). The 'No RT' control cDNAs were also included and no amplification was observed for any assay within the 40 cycles tested, indicating that the intron expression measured here was from mRNA and not amplification of contaminating genomic DNA. Each data point represents one subject (for qRT-PCR each data point represents the mean of technical triplicates). Bars show the median expression values.

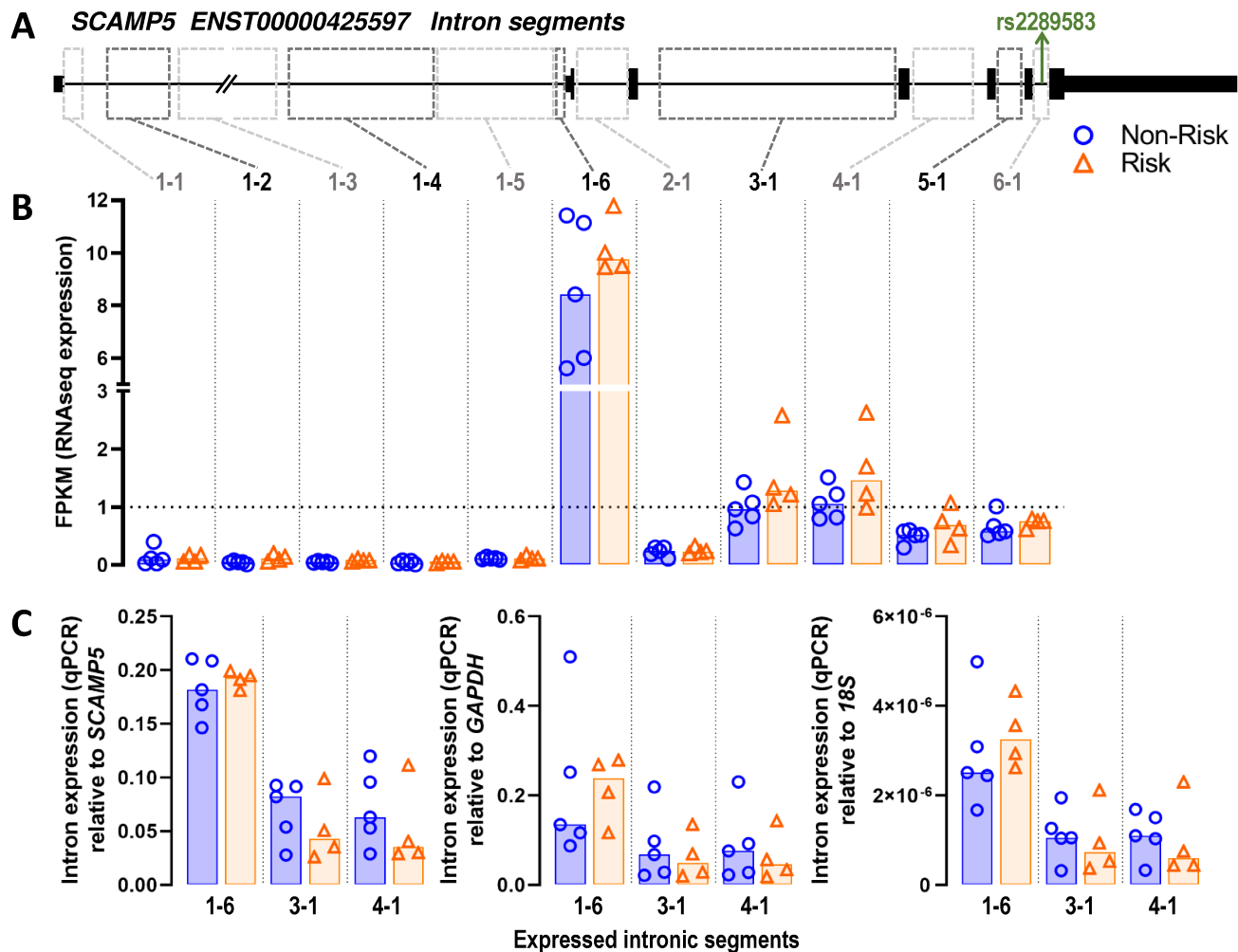


Figure S5. BDCA4 KO using CRISPR in primary human pDCs. pDCs were isolated to near purity and electroporated with Cas9 particles complexed with non-targeting or *BDCA4* gRNA A or B. Cells were cultured for 72hrs and stained for viability and BDCA4 expression prior to acquisition by flow cytometry.

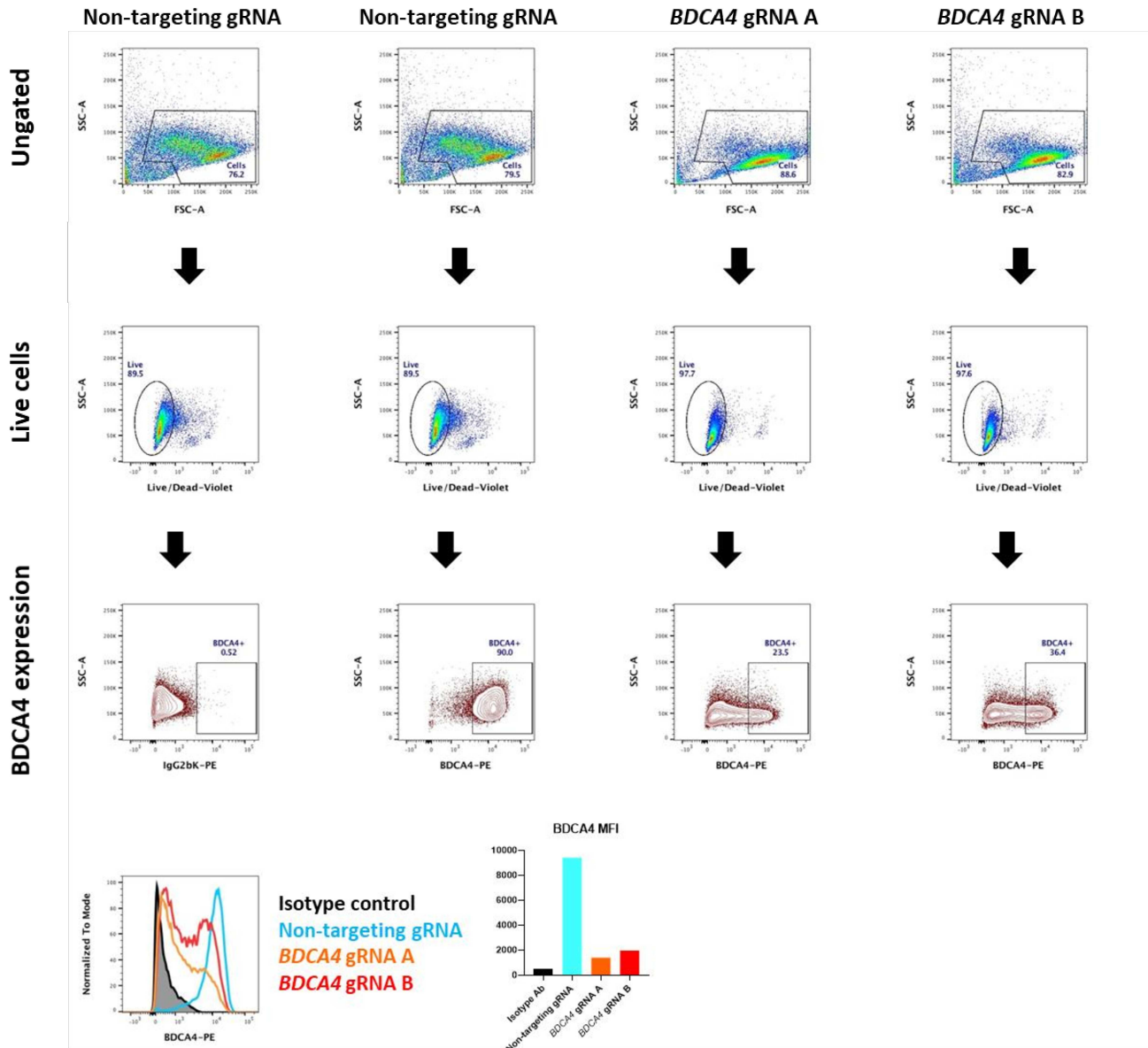


Figure S6. Representative pre- and post-isolation purity of pDCs from recalled GaP subjects.

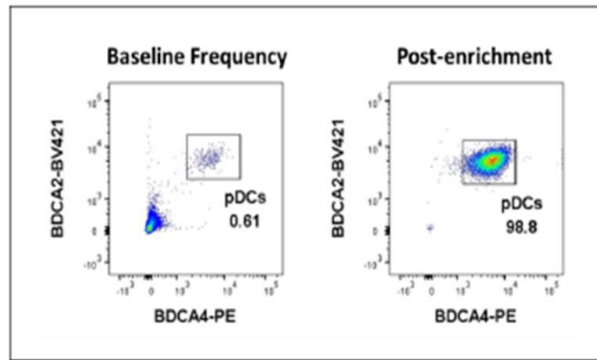


Table S1. Construction of an SLE risk haplotype about rs2289583.

	rs2472300	rs6495122	rs2289583*	Number of subjects		Frequency		P value	OR (95% CI)
				Controls	SLE	Controls	SLE		
Non-risk	G	C	C	6,324	3,404	45.4%	42.2%	2.5x10 ⁻⁶	0.88 (0.83 - 0.93)
Risk	A	A	A	2,508	1,645	18.0%	20.4%	1.8x10 ⁻⁵	1.16 (1.09 - 1.25)
	G	A	C	1,953	1,137	14.0%	14.1%	0.92	1.00 (0.93 - 1.09)
	A	A	C	1,286	780	9.2%	9.7%	0.30	1.05 (0.96 - 1.15)
	G	C	A	957	548	6.9%	6.8%	0.82	0.99 (0.88 - 1.10)
	G	A	A	545	355	3.9%	4.4%	0.084	1.13 (0.98 - 1.29)
	A	C	C	300	174	2.2%	2.2%	1.00	1.00 (0.83 - 1.21)
	A	C	A	45	29	0.3%	0.4%	0.72	1.11 (0.70 - 1.77)
				13,918	8,072				

Table S2. Characteristics of GaP subjects recalled for pDC isolation.

Subject	Sex Assigned at Birth:	Race	Medical Conditions	SCAMP5 Haplotype	pDC Frequency Pre-Enrichment	pDC yield	pDC purity
3333	Female	Caucasian	None	Non-Risk	0.60%	4.55E+05	97.00%
3538	Female	Caucasian	Hypothyroidism	Non-Risk	0.40%	3.18E+05	97.70%
4315	Female	Caucasian	None	Non-Risk	0.44%	2.18E+05	95.10%
4752	Female	Caucasian	Allergies	Non-Risk	0.11%	3.55E+04	86.10%
4855	Female	Caucasian	Eczema	Non-Risk	0.39%	2.35E+05	96.50%
4892	Female	Caucasian	Allergies, Asthma	Non-Risk	0.36%	8.50E+04	97.40%
5121	Female	Caucasian	Allergies	Non-Risk	0.75%	4.43E+05	95.00%
5135	Female	Caucasian	Psoriasis	Non-Risk	0.73%	2.10E+05	98.20%
5444	Female	Caucasian	Allergies	Non-Risk	0.44%	1.45E+05	95.80%
6845	Female	Caucasian	None	Non-Risk	0.64%	2.56E+05	98.60%
7101	Female	Caucasian	None	Non-Risk	0.78%	3.00E+05	92.70%
7153	Female	Caucasian	None	Non-Risk	0.13%	1.56E+05	93.20%
7170	Female	Caucasian	Allergies, Asthma, Arthritis	Non-Risk	0.41%	1.20E+05	94.50%
7644	Female	Caucasian	Arthritis, Diabetes Type 1, Psoriasis	Non-Risk	1.94%	5.85E+05	98.60%
7738	Female	Caucasian	Allergies, Hypothyroidism	Non-Risk	0.53%	1.60E+05	97.70%
2727	Female	Caucasian	None	Risk	0.25%	1.13E+05	93.70%
3425	Female	Caucasian	None	Risk	0.74%	4.20E+05	97.80%
5050	Female	Caucasian	Allergies	Risk	0.62%	3.13E+05	98.80%
5181	Female	Caucasian	None	Risk	0.63%	2.32E+05	97.10%
5451	Female	Caucasian	None	Risk	0.44%	2.19E+05	98.60%
6257	Female	Caucasian	Celiac Disease	Risk	0.61%	9.18E+04	96.70%
6335	Female	Caucasian	None	Risk	0.46%	2.23E+05	97.70%
7450	Female	Caucasian	None	Risk	0.79%	3.00E+05	97.70%
7992	Female	Caucasian	None	Risk	0.68%	4.40E+05	98.00%

Videos 1-4. Intracellular trafficking of SCAMP5-bearing vesicles in transduced HEK cells.

Videos 5-7. Time-lapse imaging of c-mVenus, IFNsp-mVenus and SCAMP5 in transduced HEK cells.